Proceeding of the IEEE
International Conference on Robotics and Biomimetics
Dali, China, December 2019

Localizability of Laser SLAM Robot Based on Deep Learning*

Zhaojian Li, Yang Gao, Shuqi Wang, Jiang Liu
School of Automobile
Chang'An University
Xi'an, China
15553507396@163.com, nchygy@126.com, w18209261604@163.com, tust1314@126.com

***Abstract* - Positioning is the key technology in the field of mobile robot, and it is also the basis of various tasks such as autonomous movement. Localizability is a measure of the ability to achieve accurate positioning for a given location, and it is an important indicator to further avoid positioning failure in upper tasks. Taking the fusion positioning method based on map matching and trajectory estimation as the research object, this paper analyses its working mechanism, designs different neural networks for different positioning methods, and proposes a neural network model composed of convolutional neural network, recurrent neural network and multi-layer perceptron. The model can be used for mobile robot estimate localizability. The simulation and experimental results show that the model can accurately estimate the localizability of the robot in a given map.**

Keywords - localizability; neural network; mobile robot; location entropy.

I. INTRODUCTION

Mobile robot has broad application prospects in industrial manufacturing, medical service, exploration and other fields. Its movement, environment exploration and other tasks are highly dependent on accurate posture estimation, that is, positioning results. At present, the commonly used positioning methods in the field of mobile robots include map matching, satellite positioning, inertial navigation, track estimation and so on. However, in reality, there are various environments that are difficult to achieve accurate positioning. For example, in an empty environment or a long and narrow corridor, it is difficult to achieve accurate positioning by relying on map matching. How to reasonably avoid entering such an environment is a major difficulty faced by mobile robots. Localizability refers to the degree of difficulty for mobile robots to obtain accurate positioning, and also specifies the size of position error. This paper takes the commonly used location algorithm based on map matching and track estimation as the research object, and analyses the localizability evaluation method under given map conditions, which provides the basis for mobile robot to achieve effective path planning and autonomous mobile.

As an important research field of robot technology, localizability estimation has been studied by many scholars in recent years, and its evaluation results have been used successfully to control the robot to achieve more effective motion. Sun proposed a reliable self-localization method for mobile robot with RGB-D sensor assisted laser sensor [1], Zhen proposes a robust positioning method that combines the measurement of inertial measurement unit (IMU) and rotating laser scanner. In addition, a new method for evaluating the localizability of a given three-dimensional map is proposed [2], Qian proposes and implements a localization estimation method for multi-sensor observations. The contribution of this method is to estimate the dynamic positioning matrix in the framework of probability by combining noise laser ranging data and RGB-D data [3], Liu proposed an off-line localizability estimation method based on known probability grid graph (PGM), and gave a localizability matrix describing the characteristics of expected location probability distribution (LPD) [4], Wang proposed an improved particle filter localization algorithm based on localization estimation. For one thing, the algorithm uses the localizability matrix of the observation model to estimate the confidence of the laser rangefinder observation. For another thing, the covariance matrix of the prediction model is used to estimate the confidence of odometer data [5], Ferreira proposes an adaptive information fusion neural network framework B-PR-F based on heuristic algorithm, which evaluates the confidence of a single estimate before fusing information [6], Wang proposed a location estimation method for mobile robots. This method transforms Fisher matrix of robot location into discrete form, and obtains static location matrix of off-line estimation. The static positioning matrix is modified by local perception influence factor, and a dynamic positioning matrix is proposed for online estimation [7]. Alomari introduces a static path planning model for mobile anchor assisted positioning in wireless sensor. Compared with similar static models, this model can estimate its position with higher positioning accuracy [8]. Chen proposed a particle filter localization algorithm based on localizability to maintain the positioning accuracy of mobile robots in highly enclosed and dynamic environments [9]. Yang, Z discusses how mobility assists localization with respect to enhancing location accuracy, decreasing deployment cost, and enriching location context [10]. Wu, HJ proposes an efficient distributed method, which is superior to the existing algorithms in terms of time delay and accuracy of location detection [11]. In [12], localizability is

* This work is partially supported by CNSF Grant #61503043, Central university fund #3100102229103, Natural science foundation of shaanxi province # 2019JLP-07 and Central university fund #300104292209 to Yang Gao.

978-1-7281-6321-5/19//$31.00 ©2019 IEEE

defined to evaluate the observations according to the prior-map (probabilistic grid map) and observation (laser range-finder) models based on the Cramer-Rao Bound. In order to improve the robot positioning ability, Ruiz-Mayor proposes an ambiguity model independent of the robot navigation system [13]. In [14], a novel localizability judgment method for UWSNs is proposed based on rigidity theory. Li, F proposes a method measuring the confidence in the information provided by the positioning system using a metric called Map Aided Horizontal Uncertainty Level (MA-HUL) [15]. Hu, C proposes an approach to uncertainty optimal path planning for a mobile manipulator based on localizability and guarantee manipulability simultaneously. Information matrix is used to indicate the localizability or localization uncertainty in a known map [16]. In order to improve the reliability of positioning, Fankhauser, P proposes a novel terrain mapping method, which bases on proprioceptive localization from kinematic and inertial measurements only [17]. In [18], a Robust Component Generation and Realization (RCGR) algorithm is developed, which generates components based on the robustness metrics. RCGR has better noise resistance and positioning accuracy. In [19], an indoor cooperative localization and tracking algorithm (CLTA) based on grid is developed, which is better than single network localization algorithm on localization and tracking performance. In [20], Schloemann, J mathematically characterizes the improvement in device localizability achieved by allowing collaboration among devices. Bhandari, T derives a mathematically tractable expression for localizability probability, where localizability is defined as the union of the two events [21]. Le Ny, J describes gradient descent-based motion planners for the robots that attempt to optimize or constrain different variations of the network's localizability function [22].

II. METHOD

At present, laser sensor is a common method of environmental perception in map matching based positioning method. There are many studies on it in the research of localizability. The commonly used localizability methods are shown below.

Assuming that the *i*-th laser data is (r_i, θ_i) by laser scanner at position s, the estimation of $s(x, y, \phi)$ by location algorithm is $\ddot{s}$, and generally assuming that $\ddot{s}$ obeys normal distribution $\hat{s} \sim N(\bar{s}, \delta_s)$, where $\bar{s}$ is its expectation, then the laser observation model can be obtained as follows. Among them, the ε is one dimensional zero mean Gaussian observation noise.

$$r_i(s) = f(s, \theta_i) + \varepsilon \tag{1}$$

$$r_i(\hat{s}) - \varepsilon = f(\hat{s}) + \frac{\partial f}{\partial s}(\hat{s} - s) \tag{2}$$

The equation (2) can be obtained by expanding the first-order Taylor series at $\bar{s}$. From $\ddot{s}$ obeying normal distribution, it is not difficult to get δ_s obeying (3), among them, $\mathrm{var}()$ function is to take variance of input random variables. Because $\frac{\partial f(\hat{s}, \theta)}{\partial s}$ is a 1×3 vector rather than a matrix, it is impossible to get $\sum$ directly by (3). Considering that the left side of (3) is the compression of δ_s from 3×3 matrix to 1 dimension, (4) can be obtained by calculating the entropy on both sides of (3), where $H()$ is the function of calculating the entropy. From the definition of continuous entropy, the location entropy can be obtained as shown in (5).

$$\left(\frac{\partial f(\hat{s}, \theta)}{\partial s}\right)\delta\left(\frac{\partial f(\hat{s}, \theta)}{\partial s}\right)^T = \mathrm{var}(r_i - \varepsilon) \tag{3}$$

$$\begin{aligned} H(r_i) + H(\varepsilon) &= \frac{1}{2}\ln\left(\left|2\pi e \delta_s\right| \left|\frac{\partial f}{\partial s}\frac{\partial f}{\partial s}^T\right|\right) \\ &= \frac{1}{2}\ln(\left|2\pi e \delta_s\right|) + \frac{1}{2}\ln\left(\left|\frac{\partial f}{\partial s}\frac{\partial f}{\partial s}^T\right|\right) \end{aligned} \tag{4}$$

$$H(\hat{s}) = H(r_i) + H(\varepsilon) - \frac{1}{2}\ln\left(\left|\frac{\partial f}{\partial s}\frac{\partial f}{\partial s}^T\right|\right) \tag{5}$$

Because the localization of robots is actually the result of fusion of estimates obtained from all observations. Therefore, the same state is estimated according to the information fusion theory. Assuming that the estimators are independent, the fused estimation results can be obtained as shown in (6). Furthermore, the entropy after fusion is shown in (7).

$$\hat{\delta}_s = \left(\frac{1}{N}\sum_{i=1\cdots N}(\delta_s)^{-1}\right)^{-1} \tag{6}$$

$$H(\hat{s}) = \frac{1}{2}\ln\left(\left|2\pi e\left(\frac{1}{N}\sum_{i=1\cdots N}(\hat{\delta}_s)^{-1}\right)^{-1}\right|\right) \tag{7}$$

III. JOINT NEURAL NETWORK MODEL

In this paper, we build a neural network model named joint neural network model to estimate the localizability (entropy) of the robot. The joint neural network model consists of three different neural networks: convolutional neural network, recurrent neural network and multi-layer perceptron. As shown in Fig. 1, $\mathbf{X}_1(t)$ is estimated to be $S_1(t)$ through the convolutional neural network and $X_2(t)$, $X_3(t)$, $S(t\text{-}1)$ is estimated to be $S_2(t)$ through the recurrent neural network, the input of the multi-layer perceptron is $S_1(t)$, $S_2(t)$ and the output is $S(t)$. Among them, $\mathbf{X}_1(t)$ is the laser data at time *t*, and the size is 1×1080 vector, $X_2(t)$ is the distance travelled by the robot at time *t-1 ~ t*, $X_3(t)$ is the Angle that the robot rotates at time *t-1 ~ t*, $S_1(t)$, $S_2(t)$ is the estimated entropy of convolutional neural network and recurrent neural network at time *t* and $S(t\text{-}1)$, $S(t)$ is the entropy at the corresponding time.

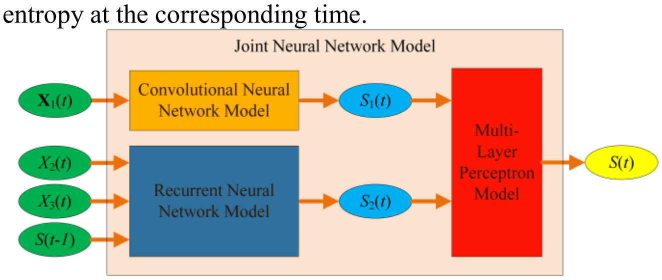

Fig. 1 Structure of joint neural network model.

A. Convolutional neural network model

Because the estimation function of location entropy such as formula is too complex, it is difficult to calculate the location estimation entropy directly after fusion. Therefore, the convolutional neural network is designed as shown in Fig. 2. Considering that entropy and $\frac{\partial f}{\partial s}$ as shown in (5), that is, there is a relationship between the magnitude of the slope at the observation point, and such slope change may exist in multiple places in a single observation data. Therefore, this paper uses Convolutional Neural Networks (CNN) architecture.

As shown in Fig. 2, the input layer of the neural network is directly connected to the distance observation value of the surrounding environment map at a given point. Because the purpose of the neural network in this paper is to estimate the location entropy, it belongs to the regression problem. Therefore, only one neuron is used in the output layer, and the activation function is a linear function. There are 36 layers in the hidden layer design, including 6 convolutional layers and 30 hidden layers. The first three convolutional layers have 1024 convolutional cores in each layer, and the last three convolutional layers have 512 convolutional cores in each layer. The size of convolutional cores in each layer is the same as that of input data in each layer. The activation function of convolutional layer is a Rectified Linear Unit. There are 1024 neurons in the hidden layer 1~5, 512 neurons in the hidden layer 6~10, 1024 neurons in the hidden layer 11~15, 256 neurons in the hidden layer 16~20, 512 neurons in the hidden layer 21~25 and 256 neurons in the hidden layer 26~30. The activation functions are linear rectifier functions.

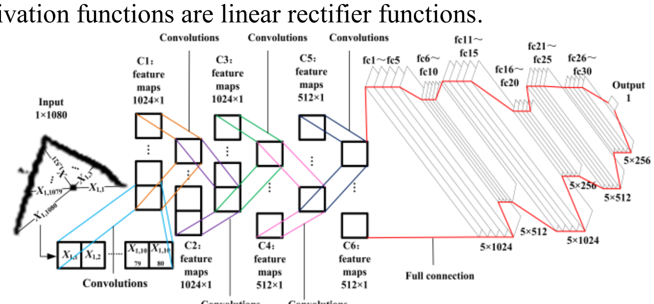

Fig. 2 Structure of convolutional neural network.

B. Recurrent neural network model and multi-layer perceptron

The robot's displacement, rotation angle in a period of time and entropy have a strong time correlation. Recurrent neural network is a good model for predicting time series data. There are ten Long Short-Term Memory (LSTM) layers, the output size of the first LSTM layer is 3×1 vector, LSTM layer 2 ~ 10 output size is 50×1 vector, the output layer has one neuron, and the activation function is a linear function. The structure of recurrent neural network is shown in Fig. 3.

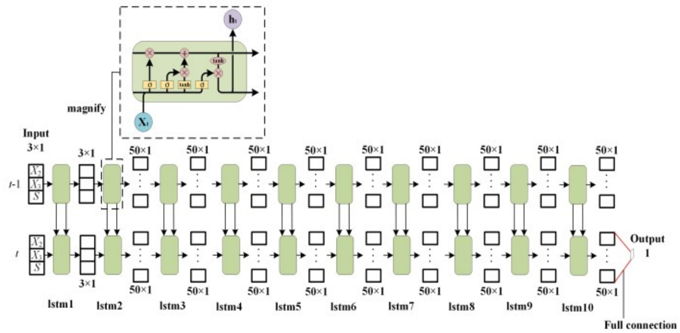

Fig. 3 Structure of recurrent neural network.

There is a mapping relationship between the output of convolutional neural network and recurrent neural network and the output of joint neural network model. This paper uses multi-layer perceptron to fit the relationship between them. The multi-layer perceptron has five hidden layers, the first two hidden layers have 256 neurons, the hidden layer 3 and the hidden layer 4 have 128 neurons, the last hidden layer has 64 neurons, the activation function of the hidden layer is a linear rectification function (Rectified Linear Unit), the output layer has one neuron, and the activation function is a linear function. The structure of multi-layer perceptron is shown in Fig. 4.

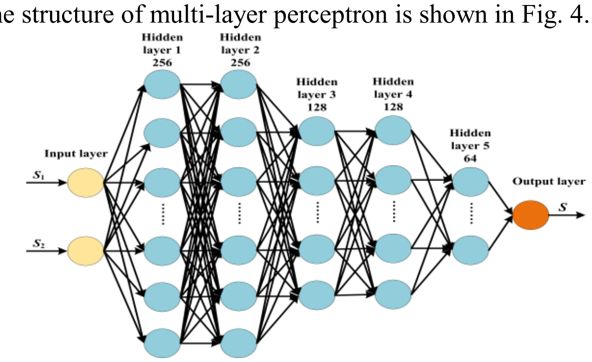

Fig. 4 Structure of multi-layer perceptron.

IV. EXPERIMENT

A. Data collection and production

In this paper, data acquisition experiments are made for common indoor and outdoor environments. Pioneer P3DX robot and Hokuyo UTM-30LX Lidar are used for data acquisition platform. The scanning angle range of the Lidar is 270°, the angular resolution is 0.25°, and the maximum detection distance is set to 30 meters, as shown in Fig. 5. The type of experimental environment and the amount of data are shown in Table 1. AMCL algorithm is used in the localization algorithm. Each group of data includes time stamp, laser scanning data, linear velocity, angular velocity and location entropy.

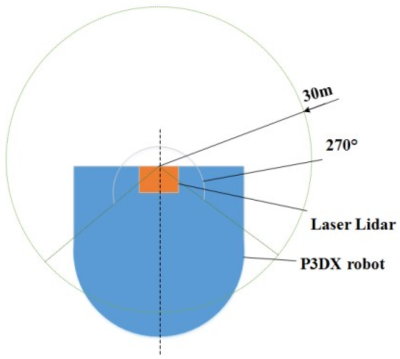

Fig. 5 Laser scanning schematic diagram.

TABLE I
DATA COLLECTION TYPE AND DATA VOLUME DISTRIBUTION

Site type	Square ground	outd- -oor scenes	Indoor long corridor	Extensive outdoor scenes	Round ground	Trian- -gular ground
Data volume (group)	854	854	3871	4013	1069	1790
Total number (group)	12451					

In this paper, the whole data set is divided into A and B data sets, which are used to train convolutional and recurrent neural networks respectively. Data set A consists of laser scanning data and location entropy, which are used as input and output of convolutional neural network respectively. Data set B needs to be preprocessed. The processing method is to calculate the difference between the current timestamp and the previous timestamp, and multiply the difference by the linear velocity and angular velocity under the current timestamp to obtain the robot's line displacement and angular displacement. Data set B is composed of line displacement, angular displacement and location entropy. Among them, the current timestamp line displacement, angular displacement and the previous timestamp location entropy are the input of recurrent neural network, and the current timestamp location entropy is the output of this network. In addition, the whole data set is normalized.

The location entropy of the whole data set is between [-11.57, 10.46]. In order to observe the distribution of location entropy of the whole data set conveniently, the range of location entropy is redefined [-12, 11]. In this paper, location entropy is divided into 23 intervals according to the range of 1. The number of location entropy in each interval is shown in Fig. 6. From Fig. 6, we can see that small and large entropy values occupy a small proportion in this data set, about 3.2% of the entire data set.

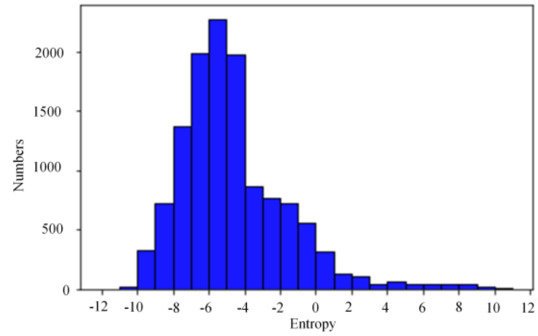

Fig. 6 Entropy distribution map.

Before training, data sets need to be partitioned. In this paper, the whole data set is divided into train set, validation set and test set. If the train set is too small, the model will not be fully trained, and the model will not achieve satisfactory results; if the train set is too large, the test set will be too small, so the effect of the model is not accurately tested. In this paper, the whole data set is divided into 64% train set, 16% validation set and 20% test set.

B. *Model Training and Testing*

Firstly, the convolutional neural network is trained separately. The training method adopts back propagation learning algorithm. The batch size is set to 20, epoch is set to 5000, the learning efficiency coefficient is set to 0.002, and the loss function adopts mean square error. After training, the weight is saved. Loss curve of convolutional neural network on train set and validation set is shown in Fig. 7. After training for 5000 times, the result of train set is shown in Fig. 8, the horizontal axis of the figure is the real value of location entropy, and the vertical axis is the estimated value of convolutional neural network. The average error of train set and validation set is 0.00056 and 0.00380 respectively. The average error of the test set is 0.00387 as shown in Fig. 9.

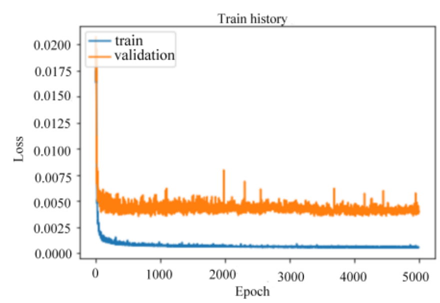

Fig. 7 Convolutional neural network loss curve.

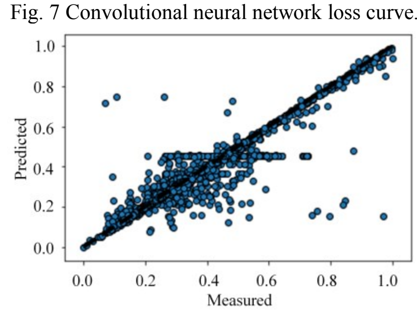

Fig. 8 Convolutional neural network train results.

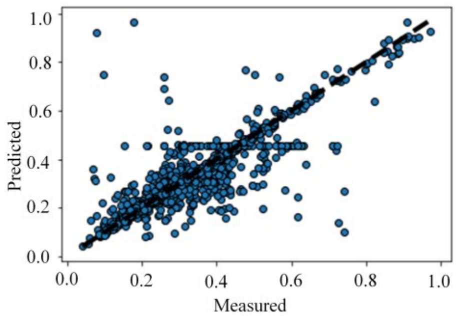

Fig. 9 Convolutional neural network test results.

Then the recurrent neural network is trained separately, using the same super parameters as convolutional neural network, and the weight is saved after the training. Loss curves on train set and validation set of recurrent neural network are shown in Fig. 10. The result of the train set is shown in Fig. 11 with an average error of 0.00066. The average error of the validation set is 0.00240. The test result of the test set is shown in Fig. 12 with an average error of 0.00027.

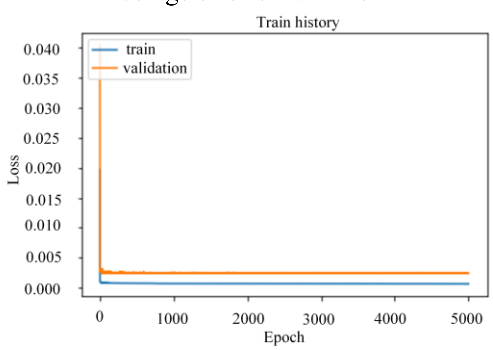

Fig. 10 Recurrent neural network loss curve.

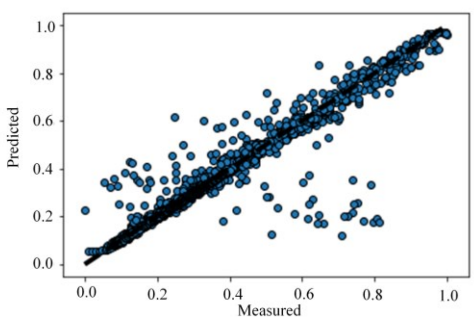

Fig. 11 Recurrent neural network train results.

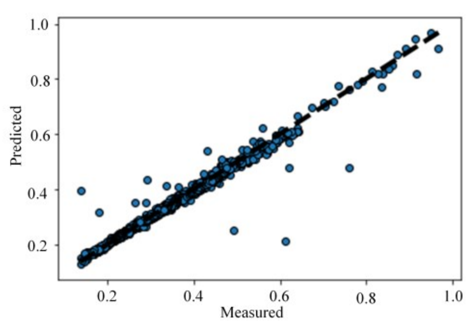

Fig. 12 Recurrent neural network test results.

Finally, the weights of convolutional neural network and recurrent neural network are loaded to train joint neural network model. The weights of multi-layer perceptron are updated only without updated the weights of convolutional neural network and recurrent neural network. The super parameters are the same as convolutional neural network. Loss curves on training set and validation set of joint neural network model are shown in Fig. 13. The result of the training set is shown in Fig. 14 with an average error of 0.00021. The average error of the validation set is 0.00160. The test result of the test set is shown in Fig. 15 with an average error of 0.00050.

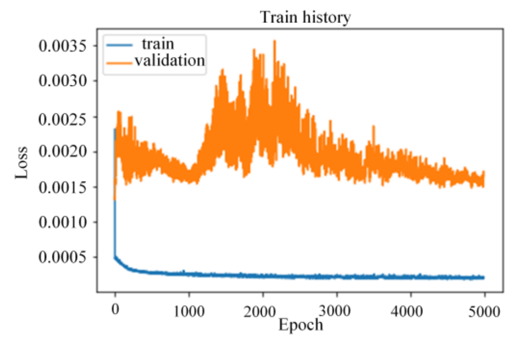

Fig. 13 Joint neural network model loss curve.

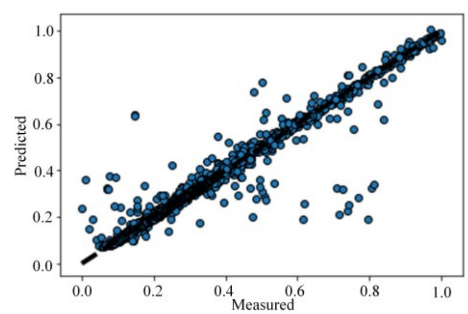

Fig. 14 Joint neural network model train results.

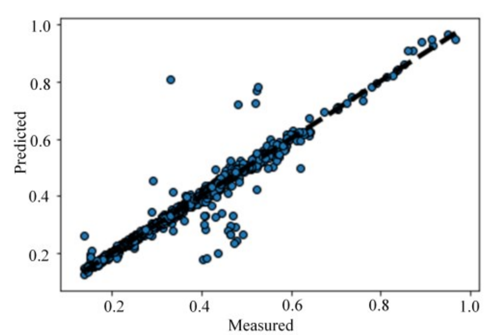

Fig. 15 Joint neural network model test results.

In order to verify the effect of the model in this paper, the model is used in the localization estimation experiment in a new environment where data has never been collected. The overall environment of the experiment is shown in Fig. 16. The experimental results of the model are shown in Fig. 17 with an average error of 0.00277.

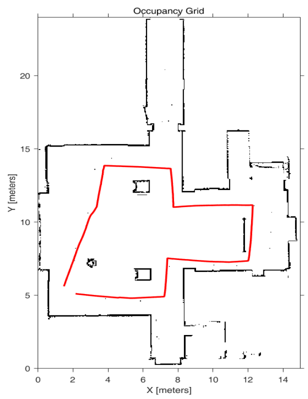

Fig. 16 Map of experimental environment.

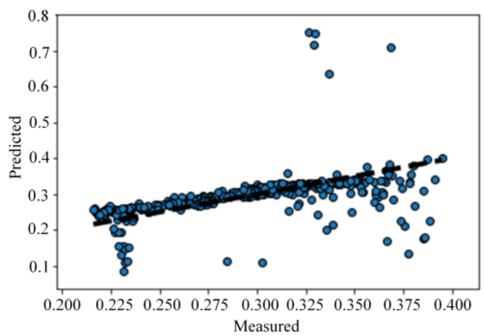

Fig. 17 Experimental result.

V. Conclusion

This paper proposes a localizability evaluation method for mobile robots based on deep learning. Based on the analysis of the location error in map matching, the location entropy is chosen to represent the localizability. According to the analysis results, a neural network model composed of convolutional neural network, recurrent neural network and multi-layer perceptron is designed to estimate the location entropy. The experimental results show that the neural network model designed in this paper can obtain a relatively accurate estimation effect, and the error is less than 2.26% compared with the measured entropy.

References

[1] Sun, Z. F., Qian, K., Ma, X. D. and Dai, X. Z., "Self-localization of mobile robot in dynamic environments based on localizability estimation with multi-sensor observation," CAAI Transactions on Intelligent Systems, 2017. 12(4): p. 443-449.

[2] Zhen, W. K., Zeng, S. and S. Soberer, "Robust localization and localizability estimation with a rotating laser scanner," in 2017 IEEE International Conference on Robotics and Automation. 2017. p. 6240-6245.

[3] Qian, K., Ma, X. D., Fang, F., Dai, X. Z. and Zhou, B., "Mobile robot self-localization in unstructured environments based on observation localizability estimation with low-cost laser range-finder and RGB-D sensors," International Journal of Advanced Robotic Systems, 2016. 13.

[4] Liu, Z., Chen, W. D., Wang, J. C. and Wang, H. S., "Action Selection for Active and Cooperative Global Localization based on Localizability Estimation," 2014 Ieee International Conference on Robotics and Biomimetics Ieee-Robio 2014, 2014: p. 1012-1018.

[5] Wang Y., Chen W. D., Wang J. C. and Wang W., "Improved Particle Filter Localization in Crowded Environments for Mobile Robots," Robot, 2012. 34(5): p. 596-603.

[6] H. Ferreira Chame, M.M. dos Santos, and S.S. da Costa Botelho, "Neural network for black-box fusion of underwater robot localization under unmodeled noise," Robotics and Autonomous Systems, 2018. 110: p. 57-72.

[7] Wang, W., W. Chen, and Y. Wang, "Probabilistic Grid Map Based Localizability Estimation for Mobile Robots," Robot, 2012. 34(4): p. 485-91, 512.

[8] A. Alomari, F. Comeau, W. Phillips, and N. Aslam, "New path planning model for mobile anchor-assisted localization in wireless sensor networks," Wireless Networks, 2018. 24(7): p. 2589-2607.

[9] Wang, Y., Chen, W. D. and Wang, J. C., "Map-based localization for mobile robots in high-occluded and dynamic environments," Industrial Robot: the international journal of robotics research and application, 2014. 41(3): p. 241-252.

[10] Yang, Z., Wu, C. S., Zhou, Z, M., Zhang, X, L., Wang, X. and Liu, Y. H., "Mobility Increases Localizability: A Survey on Wireless Indoor Localization using Inertial Sensors," ACM Comput. Surv., 2015. 47(3): p. 1-34.

[11] Wu, H., Ding, A., Liu, W., Li, L. Z and Yang, Z., "Triangle Extension: Efficient Localizability Detection in Wireless Sensor Networks," IEEE Transactions on Wireless Communications, 2017. 16(11): p. 7419-7431.

[12] Wang, Y., Chen, W. D., Wang, J. C. and Wang, H. S., "Active global localization based on localizability for mobile robots," Robotica, 2015. 33(8): p. 1609-1627.

[13] A. Ruiz-Mayor, J. C. Crespo, and G. Trivino, "Perceptual ambiguity maps for robot localizability with range perception," Expert Systems with Applications, 2017. 85(1): p. 33-45.

[14] Xia, N., Ou, Y. X., Wang, S. L., Zheng, R., Du, H. Z. and Xu, C. N., "Localizability Judgment in UWSNs Based on Skeleton and Rigidity Theory," IEEE Transactions on Mobile Computing, 2017. 16(4): p. 980-989.

[15] Li, F., P. Bonnifait, and J. Ibanez-Guzman., "Estimating localization uncertainty using multi-hypothesis map-matching on high-definition road maps," in 20th IEEE International Conference on Intelligent Transportation Systems, ITSC 2017, October 16, 2017 - October 19, 2017. 2018. Yokohama, Kanagawa, Japan: Institute of Electrical and Electronics Engineers Inc.

[16] Hu, C., Chen,W., Wang, J. and Wang, H., "Optimal path planning for mobile manipulator based on manipulability and localizability," in 2016 IEEE International Conference on Real-time Computing and Robotics (RCAR). 2016.

[17] P. Fankhauser, M. Bloesch, and M. Hutter, "Probabilistic Terrain Mapping for Mobile Robots With Uncertain Localization," IEEE Robotics and Automation Letters, 2018. 3(4): p. 3019-3026.

[18] Sun, T.Y., Wang, Y. C., Li, D. Y., Chen, W. P. and Gu, Z. Q., "Robust Component-based Network Localization with Noisy Range Measurements," 2018 27th International Conference on Computer Communication and Networks (Icccn), 2018.

[19] Luo, J., Zhang, Z. Y., Liu, C. and Luo, H. B., "Reliable and Cooperative Target Tracking Based on WSN and WiFi in Indoor Wireless Networks," IEEE Access, 2018. 6: p. 24846-24855.

[20] J. Schloemann, H. S. Dhillon, and R. M. Buehrer, "A Tractable Analysis of the Improvement in Unique Localizability Through Collaboration," IEEE Transactions on Wireless Communications, 2016. 15(6): p. 3934-3948.

[21] T. Bhandari, H. S. Dhillon, and R. M. Buehrer, "The Impact of Proximate Base Station Measurements on Localizability in Cellular Systems," 2016 IEEE 17th International Workshop on Signal Processing Advances in Wireless Communications (Spawc), 2016.

[22] J. Le Ny, and S. Chauviere, "Localizability-Constrained Deployment of Mobile Robotic Networks with Noisy Range Measurements," in 2018 Annual American Control Conference. 2018. p. 2788-2793.